LIMNOLOGY and OCEANOGRAPHY

ASLO

Limnol. Oceanogr. 9999, 2020, 1–13

doi: 10.1002/lno.11564

Metabolism overrides photo-oxidation in CO_2 dynamics of Arctic permafrost streams

Gerard Rocher-Ros,[1*] **Tamara K. Harms**,[2] **Ryan A. Sponseller**,[1] **Maria Väisänen**,[3,4] **Carl-Magnus Mörth**,[5] **Reiner Giesler**[1]

[1]Climate Impacts Research Centre, Department of Ecology and Environmental Science, Umeå University, Abisko, Sweden
[2]Institute of Arctic Biology and Department of Biology & Wildlife, University of Alaska Fairbanks, Fairbanks, Alaska
[3]Arctic Centre, University of Lapland, Rovaniemi, Finland
[4]Ecology and Genetics Research Unit, University of Oulu, Oulu, Finland
[5]Department of Geological Sciences, Stockholm University, Stockholm, Sweden

Abstract

Global warming is enhancing the mobilization of organic carbon (C) from Arctic soils into streams, where it can be mineralized to CO_2 and released to the atmosphere. Abiotic photo-oxidation might drive C mineralization, but this process has not been quantitatively integrated with biological processes that also influence CO_2 dynamics in aquatic ecosystems. We measured CO_2 concentrations and the isotopic composition of dissolved inorganic C ($\delta^{13}C_{DIC}$) at diel resolution in two Arctic streams, and coupled this with whole-system metabolism estimates to assess the effect of biotic and abiotic processes on stream C dynamics. CO_2 concentrations consistently decreased from night to day, a pattern counter to the hypothesis that photo-oxidation is the dominant source of CO_2. Instead, the observed decrease in CO_2 during daytime was explained by photosynthetic rates, which were strongly correlated with diurnal changes in $\delta^{13}C_{DIC}$ values. However, on days when modeled photosynthetic rates were near zero, there was still a significant diel change in $\delta^{13}C_{DIC}$ values, suggesting that metabolic estimates are partly masked by O_2 consumption from photo-oxidation. Our results suggest that 6–12 mmol CO_2-C m^{-2} d^{-1} may be generated from photo-oxidation, a range that corresponds well to previous laboratory measurements. Moreover, ecosystem respiration rates were 10 times greater than published photo-oxidation rates for these Arctic streams, and accounted for 33–80% of total CO_2 evasion. Our results suggest that metabolic activity is the dominant process for CO_2 production in Arctic streams. Thus, future aquatic CO_2 emissions may depend on how biotic processes respond to the ongoing environmental change.

Arctic streams and rivers are conduits for CO_2 evasion to the atmosphere (Kling et al. 1991; Stackpoole et al. 2017) that may further increase due to climate warming and the associated mobilization of carbon (C) stored in permafrost (Spencer et al. 2015; Wild et al. 2019; Zolkos et al. 2019). Organic C entering aquatic ecosystems can be converted to CO_2 through two distinct pathways: abiotically via photochemical oxidation (hereafter photo-oxidation; Granéli et al. 1996) and biotically via microbial mineralization (Tranvik 1988; Cole and Caraco 2001). In Arctic streams, photo-oxidation may contribute a large fraction of the CO_2 evaded to the atmosphere (Cory et al. 2014). Since this process is driven by sunlight, photo-oxidation should also increase stream CO_2 concentration from night to day (Bertilsson and Tranvik 2000). However, recent in situ observations of CO_2 dynamics in tundra, boreal, and alpine streams indicate net daytime uptake of CO_2 by photosynthesis (Peter et al. 2014; Crawford et al. 2016; Rocher-Ros et al. 2020). Thus, these two light-dependent processes have opposing effects on CO_2 concentrations and the balance between them will determine the change in CO_2 concentrations from day to night (Fig. 1a). Assessing diel changes in CO_2 concentrations can therefore aid in comparing the roles of biological and photochemical processing of C in Arctic freshwaters.

Photo-oxidation and microbial respiration of organic matter are typically studied in isolation, using approaches that incorporate different compartments of the stream ecosystem. These distinct approaches have likely impeded the resolution of the

*Correspondence: gerard.rocher@umu.se

Additional Supporting Information may be found in the online version of this article.

Special Issue: Biogeochemistry and Ecology across Arctic Aquatic Ecosystems in the Face of Change.
Edited by: Peter J. Hernes, Suzanne Tank and Ronnie N. Glud.

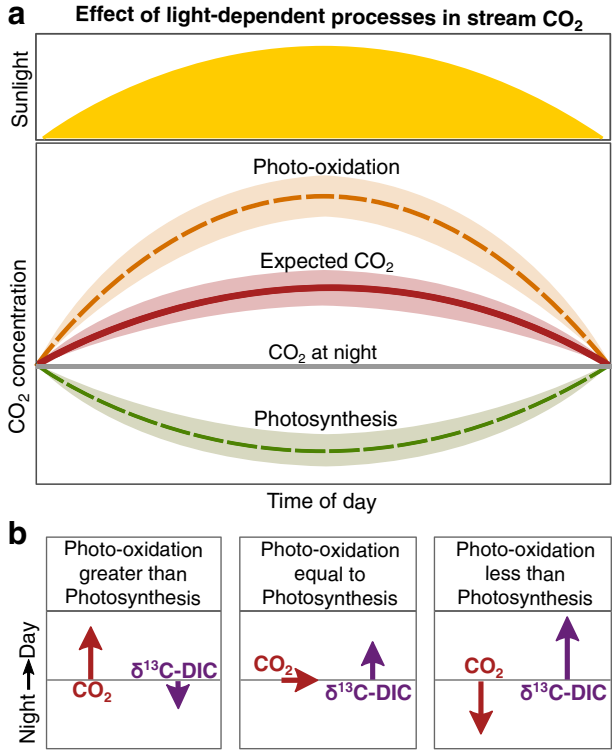

Fig. 1. Conceptual representation of the effect of light-dependent processes on dissolved CO_2 concentration in streams. (**a**) The diel change in CO_2 concentrations (red line) is the balance of two opposing processes: photo-oxidation (orange line), which produces CO_2, and photosynthesis (green line), which consumes CO_2. Panels in (**b**) describe diurnal changes in CO_2 concentration and $\delta^{13}C_{DIC}$ values resulting from three scenarios: photo-oxidation rate greater (left), equal (middle) or less (right) than photosynthesis. When photo-oxidation equals photosynthesis (middle), the isotopic effect will be determined by the latter due to a high preferential biological uptake of $^{12}CO_2$ enriching the DIC reservoir. In contrast, photo-oxidation releases $^{12}CO_2$ and $^{13}CO_2$ in the same proportion as the substrate composition. Note that this is a simplification since this effect also will depend on the reservoir size, pH and in situ isotope values.

relative influences of abiotic and biotic processes on CO_2 emissions. For example, photo-oxidation is often studied in bottles (Miller and Zepp 1995; Granéli et al. 1996; Bertilsson and Tranvik 2000; Osburn et al. 2001) and only accounts for processes in the water column. By comparison, biological metabolic rates in streams are most often assessed using open-system measures of oxygen (O_2) mass balance capturing hyporheic, benthic, and water column processes (Odum 1956; Grace et al. 2015; Hall et al. 2015; Schindler et al. 2017). Thus, to reconcile both approaches we need to evaluate the influences of photosynthesis and photo-oxidation at the ecosystem level. This can be achieved using in situ measures of the key signals and drivers of C processing (e.g., CO_2/O_2 concentrations, temperature, and light) at a temporal resolution that captures diel variation. For example, it is possible to estimate metabolic rates that affect the stream C balance—gross primary production (GPP) and ecosystem respiration (ER)—and independently compare them with dissolved CO_2 dynamics. Accordingly, photo-oxidation should generate CO_2 during the day, while GPP has an opposing effect (Fig. 1a).

Diel dynamics of dissolved inorganic C isotopes ($\delta^{13}C_{DIC}$ values) can provide complementary information to observations of O_2 and CO_2 concentrations, as photo-oxidation and photosynthesis impart contrasting effects on the $\delta^{13}C_{DIC}$ values (Fig. 1b) (Waldron et al. 2007; Giesler et al. 2013; Campeau et al. 2017). For example, past studies have shown clear diel patterns in stream $\delta^{13}C_{DIC}$ with more enriched values during daytime (Parker et al. 2005; Waldron et al. 2007), which has been explained by the high isotope fractionation of photosynthesis (Guy et al. 1993). By contrast, the isotope fractionation effect of photooxidation is generally small compared to photosynthesis and will thus only have a minor effect (Opsahl and Zepp 2001). Instead, photo-oxidation dilutes the $^{13}C_{DIC}$ reservoir toward a value of the substrate, for example, dissolved organic carbon (DOC) that is around −27‰ (Peterson et al. 1986; Campeau et al. 2017). Like photooxidation, respiration will dilute the $^{13}C_{DIC}$ reservoir toward a value similar to the organic C source respired (Giesler et al. 2013; Campeau et al. 2017). Furthermore, other processes such as degassing and carbonate weathering will increase the $\delta^{13}C_{DIC}$ values; the former due to isotopic fractionation where $^{12}CO_2$ is preferentially lost and the latter due to reservoir dilution since most carbonates are around 0‰ (Giesler et al. 2013, and references therein). Together, respiration, degassing, and weathering shape the average stream $\delta^{13}C_{DIC}$ values, yet their influence on diel patterns are most likely weak.

Given these opposing effects of photosynthesis and photo-oxidation on $\delta^{13}C_{DIC}$, we can make predictions for diel patterns depending on the relative strength of these two processes (Fig. 1b). For instance, if photo-oxidation is the dominant process, depletion of $^{13}C_{DIC}$ (leading to lighter $\delta^{13}C_{DIC}$ values) during daytime should be accompanied by higher daytime CO_2 concentrations (left panel, Fig. 1b). However, if the two processes are equal in magnitude (i.e., the same amount of C is processed by each), we would expect no diel change in CO_2 concentration but an enrichment in daytime $^{13}C_{DIC}$ (leading to heavier $\delta^{13}C_{DIC}$ values) due to a stronger effect of isotope fractionation of photosynthesis as compared the isotope dilution by photo-oxidation (middle panel, Fig. 1b). Finally, if photosynthesis dominates, we expect a distinct diel pattern with lower daytime CO_2 concentration and a clear increase in daytime $\delta^{13}C_{DIC}$ values (right panel, Fig. 1b). Using diel $\delta^{13}C_{DIC}$ values in streams may thus be helpful in disentangling the relative importance of the two light-dependent processes.

By comparing photosynthetic rates modeled using the O_2 mass balance method with independently measured diurnal variation in $\delta^{13}C_{DIC}$, it is possible to quantify the effect of photo-oxidation on whole-ecosystem estimates of C processing. Photo-oxidation consumes O_2 while producing

CO_2 (Laane et al. 1985), and therefore could mask O_2 production by photosynthesis during the day. In contrast, the diel pattern in $\delta^{13}C_{DIC}$ will be mostly driven by photosynthesis (Fig. 1b). Therefore, the relationship between photosynthetic rates and diel changes in $\delta^{13}C_{DIC}$ provides information about photo-oxidation rates. For instance, if there is a detectable diel change in $\delta^{13}C_{DIC}$ values when photosynthetic rates are zero, the amplitude of this diel change in isotopic values can be interpreted as the effect of photooxidation. However, there are several uncertainties that can influence this interpretation, such as higher daytime respiration of labile OC recently produced by photosynthesis (Hotchkiss and Hall 2014; Schindler et al. 2017) and the assumed quotient between O_2 consumed and CO_2 produced, both for respiration (Berggren et al. 2012) and photo-oxidation (Miles and Brezonik 1981). Regardless, this approach can be applied to evaluate the dominant process influencing CO_2 emissions from streams while integrating processes occurring in the water column with those that occur in benthic and hyporheic sediments (Battin et al. 2008).

The aim of this study was to assess the relative importance of light-dependent processes for CO_2 dynamics in Arctic streams that drain continuous permafrost. The Kuparuk and Toolik Rivers (Alaska) were selected due to difference in size (first and fifth order) and the existence of published estimates of photo-oxidation in this area, including an adjacent first-order stream to Toolik River (Cory et al. 2014) and the Kuparuk River. We compare published photo-oxidation rates with estimates of stream metabolism and CO_2 evasion from measured stream CO_2 and O_2 concentrations, light, and temperature. We further constrained estimates of CO_2 production by photo-oxidation using sub-daily (6-h increments) samples analyzed for alkalinity, DOC, and $\delta^{13}C_{DIC}$ values. We tested two contrasting hypotheses: (1) stream CO_2 dynamics are primarily driven by photochemical processes and (2) stream CO_2 dynamics are primarily driven by aquatic metabolism (Fig. 1). If photo-oxidation is the major driver, we predicted that CO_2 concentrations in streams would increase from night to day, when photo-oxidation rates would be greatest (Cory et al. 2014). By contrast, if GPP is the major driver, then CO_2 concentrations would decrease from night to day, when photosynthetic CO_2 fixation is greatest (Rocher-Ros et al. 2020).

Methods

Site description

We studied C cycling processes in two streams within the Kuparuk River watershed, on the North Slope of the Brooks Range in Arctic Alaska, near Toolik Field Station (Fig. S1). The climate in the upper Kuparuk watershed is characterized by a long cold season, with snow cover that spans ~ 8 months of the year. Mean annual air temperature recorded at the Toolik Field Station for the period 1989–2010 was −8.5°C (Cherry et al. 2014). The study was performed between the 18 July and 01 August 2018. Mean air temperature during the study was 13.4°C, while the historical average for this time period between 1989 and 2010 was 9.9°C. The precipitation during the study period was 63.2 mm (Fig. S2). Historically, July accounts for 44% of the annual precipitation (65 and 149 mm for July and annual precipitation respectively, for the period 1989–2010; Cherry et al. 2014). Weather data were obtained from the Environmental Data Center (Toolik Field Station, Institute of Arctic Biology 2019).

We sampled the first-order Toolik River (catchment area 5.6 km^2) and the fifth-order stream Kuparuk River (131.9 km^2; Fig. S1; Table 1). Both rivers drain tundra underlain by permafrost. Permafrost extent is continuous and soils thaw in summer to depths of 0.3 to up to 2 m, depending on topography (Shaver et al. 2014) that together indicate that water flow is mostly superficial (Rushlow and Godsey 2017) and groundwater inputs are restricted to springs (Bowden et al. 2014). Tussock tundra dominates the landscape, with patches of wet sedge and heath vegetation (Shaver et al. 2014). The riparian vegetation near streams consists of dwarf birch (*Betula nana*) and willow (*Salix spp.*), but with heights of < 1 m, streams are unshaded.

Stream measurements and sample analysis

We deployed sensors to measure physical (depth, light, temperature) and chemical (CO_2, O_2) properties at a 10-min frequency, from 18 July to 01 August 2018. Water temperature and water level were recorded by HOBO water level loggers (model U20-001-04, Onset Computer Corporation). Light intensity was monitored by HOBO MX Temperature/Light loggers (model MX2202, Onset Computer Corporation), by recording every minute and averaging to a 10-min frequency. Light intensity (in lux) was converted to photosynthetic active radiation (PAR; in μmol m^{-2} d^{-1}) using a conversion factor of 0.0185 according to Thimijan and Heins (1983). Dissolved CO_2 concentration was measured using eosGP CO_2 concentration sensors (Eosense) connected to CR1000 data loggers (Campbell Scientific). The CO_2 sensors were calibrated with standard gases in the laboratory before deployment in the field, using gas concentrations of 400, 2000, and 5000 ppm of CO_2. O_2 concentration was measured every 10 min using miniDOT oxygen sensors (Precision Measurement Engineering), fitted with a

Table 1. Catchment characteristics of the two study sites.

Site	Coordinates (WGS 1984)	Area (km^2)	Mean slope (degrees)	Elevation outlet (m)	Max. elevation (m)
Kuparuk River	68.6474, −149.4119	131.9	1.50	741	1522
Toolik River	68.6468, −149.3192	5.6	0.61	844	983

copper mesh to reduce biofouling. To verify the manufacturer-supplied calibration, we submerged sensors in oxygenated water achieved by intense bubbling for 1 h, and then logged O_2 continuously for 5 h after removing air stones, in order to reach equilibrium with the atmosphere after an initial supersaturation. We then added dry yeast and sugar to consume the dissolved oxygen. The sensors measured 100% O_2 saturation in oxygenated water and 0% after yeast and sugar was added, and therefore no further correction of observations was performed. Sensors were placed in the thalweg of each stream, with the O_2 logger facing downstream and the CO_2 sensor within in a perforated plastic pipe as a protective casing.

For the Kuparuk River, we obtained river discharge and depth from the Arctic Long-Term Ecological Research Program (http://arc-lter.ecosystems.mbl.edu). For Toolik River, discharge estimates were based on pressure measurements from HOBO water level loggers and an empirical rating curve (Fig. S3) based on five salt slug injections (Moore 2005). We used two conductivity sensors (model U24-001, Onset Computer Corporation) at separate locations during the salt releases to estimate travel time and therefore the water velocity and discharge. To assess lateral inputs of water that could affect metabolism estimates in Toolik River, we also performed multiple discharge measurements upstream (Fig. S4), but no significant inputs were detected for more than 1 km upstream. The average depth of the reach was estimated from the relationship between stream velocity (V), discharge (Q), and stream width (W): $D = Q/(W \times V)$ (Hall and Hotchkiss 2017). This reach depth was then related to the site depth measured by the pressure logger to obtain continuous estimates of the reach depth.

We collected water samples at 6-h intervals (6, 12, 18, and 24 h) for 6 d (27 July to 01 August 2018) at the same locations as the automated loggers for analysis of additional chemical constituents. We measured pH, alkalinity, and DOC from samples collected into pre-rinsed 1 liter bottles that were kept cool and subsampled in the lab within 6 h of collection. The samples for $\delta^{13}C_{DIC}$ analysis were collected with a syringe and 4 mL were injected into a 12 mL septum-sealed glass vial (Labco Limited) that had been preflushed with He gas for 3 min.

pH was measured on a 150-mL aliquot of stream water (Accumet AB pH meter, Fisher Scientific). Samples for analysis of DOC were filtered through 0.45 μm filters prerinsed with stream water (Filtropur Sarstedt), and acidified with 8 M HCl (250 μL HCl to 50 mL of stream water). DOC concentration was measured as nonpurgeable organic C by nondispersive infrared gas analysis on a total organic C analyzer (TOC-L CPH, Shimadzu Scientific Instruments; limit of quantification = 8 μM). Alkalinity was measured on 30 mL of unfiltered water collected without headspace using a Metrohm automated titration system and a Metrohm Aquatrode Plus pH electrode (Metrohm AG). The samples were titrated to pH 4.5, which is the equivalence point between H^+ and HCO_3^-, with 0.1 M HCl and alkalinity was calculated from the difference in the amount of HCl used and the sample volume. DIC was calculated from alkalinity and pCO_2 values using PHREEQCI (Parkhurst and Appelo 2013). Samples for $\delta^{13}C_{DIC}$ values determination were acidified with 100 μL of 99% H_3PO_4 as a preservative (Taipale and Sonninen 2009) and to transform all HCO_3^- and CO_3^{2-} ions to CO_2(g). $\delta^{13}C_{DIC}$ values were determined using a Gasbench II extraction line coupled to a Finnigan MAT 253 mass spectrometer. Results are given as per mil deviations from the standard (PDB) and denoted $\delta^{13}C$, and where R is the ratio of $^{13}C/^{12}C$: $\delta^{13}C_{DIC} = (R_{sample}/R_{standard} - 1) \times 10^3$. From repeated measurements of standards, the reproducibility was calculated to be better than 0.1% for $\delta^{13}C$. All samples were stored at +4°C until analyses.

Data analysis, metabolism, and CO_2 evasion

All data were analyzed using R (R Core Team 2017; version 3.5.1). The dataset with daily values and an R script to reproduce the figures and tests can be found in the Supplementary Materials. Linear regressions were performed using the *lm* function, to assess the effect of GPP on diel changes in CO_2 evasion and $\delta^{13}C_{DIC}$ values. Amplitude of diel variation in $\delta^{13}C_{DIC}$ values were calculated from the lowest and highest value within each day, whereas diel variation in CO_2 evasion was calculated as the cumulative CO_2 evasion during the light hours minus the average CO_2 evasion rate during the night. We used the O_2, temperature, light, and depth time series to model stream metabolic rates and the gas transfer velocity using the *streamMetabolizer* package (version 0.10.9). This approach models O_2 concentrations using the following equation:

$$O_{2_t} = O_{2_{t-\Delta t}} + \left(\frac{GPP}{D} \times \frac{PAR_{t-\Delta t}}{\sum_{t=0}^{t=144} PAR} \right) + \frac{ER \times \Delta t}{D} + K_{O_2} \times \left(O_{2_{sat\,(t-\Delta t)}} - O_{2_{(t-\Delta t)}} \right) \times \Delta t \quad (1)$$

where O_{2_t} is the oxygen concentration at time t (g O_2 m^{-3}), D is the channel depth (m), PAR is photosynthetically active radiation (μmol m^{-2} s^{-1}), K_{O_2} is the gas reaeration coefficient of O_2 (d^{-1}), Δt is the time step (10 min), and $O_{2_{sat}}$ is the concentration of O_2 in the water at 100% saturation. We used a Bayesian inverse model to solve for three parameters: GPP (g O_2 m^{-2} d^{-1}), ER (g O_2 m^{-2} d^{-1}), and the gas reaeration coefficient (K_{600}; d^{-1}). Prior distributions for GPP and ER were based on existing rates measured in the nearby Ivishak spring (Huryn et al. 2014), with a mean of 1 and −5 g O_2 m^{-2} d^{-1} for GPP and ER, respectively. The model was run for 10,000 iterations, and the last 500 were used as the model results. To avoid problems regarding equifinality, where multiple solutions can produce the same model fit (Appling et al. 2018), we pooled K_{600} estimates within binned categories based on stream discharge, a physical variable that should capture

variations in the turbulence regime of a river. To model K_{600}, we provided prior distributions of K_{600} for different discharge conditions. To do so, we first derived estimates of K_{600} with the night-time regression method (Hornberger and Kelly 1975) using the function *metab_night()* in *streamMetabolizer*. Figure S5 shows the initial estimates of K_{600} and the final binned $Q \sim K_{600}$ relationship obtained from the metabolism model. We compared modeled K_{600} estimates with those obtained from hydraulic measurements at Toolik River using the relationship $k_{600} = 951.5 \times (V \times S)^{0.75}$ (Raymond et al. 2012), where k_{600} is the gas transfer velocity (or $D \times K_{600}$; m d^{-1}) and S is the channel slope. The k_{600} obtained from this hydraulic relationship was similar to the values of k_{600} estimated by the metabolism model (Fig. S6).

The metabolism model in *streamMetabolizer* assumes constant ER throughout the day and estimates GPP as a linear function of light (Appling et al. 2018). This is a simplification of ecosystem processes where ER might be greater during the day (Hotchkiss and Hall 2014) due to higher temperature and/or the availability of more labile C released during photosynthesis (Schindler et al. 2017), and GPP can increase nonlinearly with light (Hanson et al. 2008). We additionally evaluated parameter estimates from BASE (Grace et al. 2015), a metabolism model that includes temperature-dependence of ER and a nonlinear relationship of GPP with light. We found that the metabolism estimates using BASE were similar to the estimates by *streamMetabolizer* (Supplementary Text S1) and we therefore report metabolic rates estimated by the more parsimonious *streamMetabolizer* model.

CO_2 exchange with the atmosphere (E_{CO_2}) was calculated as:

$$E_{CO_2} = K_{CO_2} \times D \times \left([CO_2]_w - [CO_2]_a\right) \quad (2)$$

where K_{CO_2} is (d^{-1}) is the gas reaeration coefficient obtained by the *streamMetabolizer* model, D is the channel depth (m), $[CO_2]$ is the concentration of CO_2 measured in the water (w) or in equilibrium with the atmosphere (a) (mol m^{-3}) (Raymond et al. 2012). We used an atmospheric CO_2 concentration of 390 ppm, obtained from several air CO_2 measurements performed in the field with a hand-held CO_2 sensor (Vaisala DM70). The average atmospheric pCO_2 measured for the same period in the NOAA observatory of Point Barrow (~ 400 km from study site), was 397 ppm (https://www.esrl.noaa.gov/gmd/obop/brw/). To compare CO_2 consumed by GPP with observed CO_2 emissions, we assumed that 1 mol of O_2 is exchanged by 1 mol of CO_2 (Demars et al. 2016).

Results

Chemical and physical attributes of the streams

The study streams were supersaturated in CO_2 relative to the atmosphere. The partial pressure of dissolved CO_2 (pCO_2) was 925 ± 3 ppm in the Kuparuk River and 1878 ± 16 ppm in the Toolik River (mean ± 95% confidence interval). In contrast, both streams were undersaturated in O_2 (Figs. 2, 3). The DOC concentration was lower in the Kuparuk River compared to the Toolik River, with a mean of 0.33 ± 0.02 and 0.86 ± 0.01 mmol C L^{-1}, respectively. Bicarbonate (HCO_3^-) concentration in the Kuparuk River was 0.33 ± 0.02 mmol C L^{-1} while in the Toolik River was 0.11 ± 0.01 mmol C L^{-1} over the measurement period. Isotope values, $\delta^{13}C_{DIC}$, in the Kuparuk River were −9.9 ± 0.3‰ while in the Toolik River were −14.5 ± 0.7‰. The physical properties of both streams are summarized in Table 2.

Temporal patterns in stream chemistry

Both the Kuparuk and Toolik Rivers generated diel variation in CO_2, O_2, and $\delta^{13}C_{DIC}$ values. CO_2 concentration consistently decreased from night to day, while O_2 saturation increased and $\delta^{13}C_{DIC}$ values increased during daytime. The diel changes in dissolved CO_2 concentration in the Toolik River (Fig. 3) averaged 17.4 mmol C m^{-3} (436 ppm CO_2), and ranged between 14.5 and 21.3 mmol C m^{-3}. In the Kuparuk River (Fig. 2), the mean diel change in pCO_2 was 5.4 mmol C m^{-3} (85 ppm CO_2) ranging between 2.7 and 8.2 mmol C m^{-3}. Mean diel amplitude of $\delta^{13}C_{DIC}$ values in the Toolik River was 2.9‰ (range = 2.4–4.3‰), while in the Kuparuk River was 1.4‰ (range = 1.2–2.1‰). O_2 saturation in the Toolik River had a mean diel change of 7.3% (range = 4.5–12.4%), and in Kuparuk the mean diel change was 2.4% (range = 1.6–4.1%).

Discharge was highest at the beginning of the study period and thereafter decreased until 27 July. A flood occurred 27–31 July, increasing discharge from 1.36 to 8.32 m^3 s^{-1} in the Kuparuk River and from 0.05 to 0.48 m^3 s^{-1} in the Toolik River (Figs. 2, 3). The increased flow rates coincided with dilution of HCO_3^- in both streams (Figs. 2, 3) whereas a decrease in CO_2 concentration was apparent only in the Toolik River (Fig. 3). Water temperature followed a similar pattern to air temperature (Fig. S2), with lower temperatures at the beginning of the sampling period.

Metabolic rates and CO_2 evasion

The average rate of GPP was nearly fourfold greater in the Toolik River (14.2 ± 7.9 mmol C m^{-2} d^{-1}; mean ± SD; n = 13 d) compared to the Kuparuk River (3.1 ± 2.9 mmol C m^{-2} d^{-1}, n = 11 d). GPP was positively correlated with the diel change in CO_2 evasion with a slope less than 1 (slope = 0.38; Fig. 4a). GPP was also positively correlated with the diel change in $\delta^{13}C_{DIC}$ values (R^2 = 0.98; Fig. 4b). In the Toolik River, the mean diel change in CO_2 evasion was 60.3% lower when compared to mean GPP (Fig. 5). In the Kuparuk River, both GPP and the diel CO_2 change were smaller than in the Toolik River, and diel variation in CO_2 evasion was 75.3% of mean GPP (Fig. 5).

In contrast to the patterns of GPP, ER was greater in the Kuparuk River (−263 ± 51 mmol C m^{-2} d^{-1}) than in the Toolik River (−75 ± 55 mmol C m^{-2} d^{-1}) over the observation

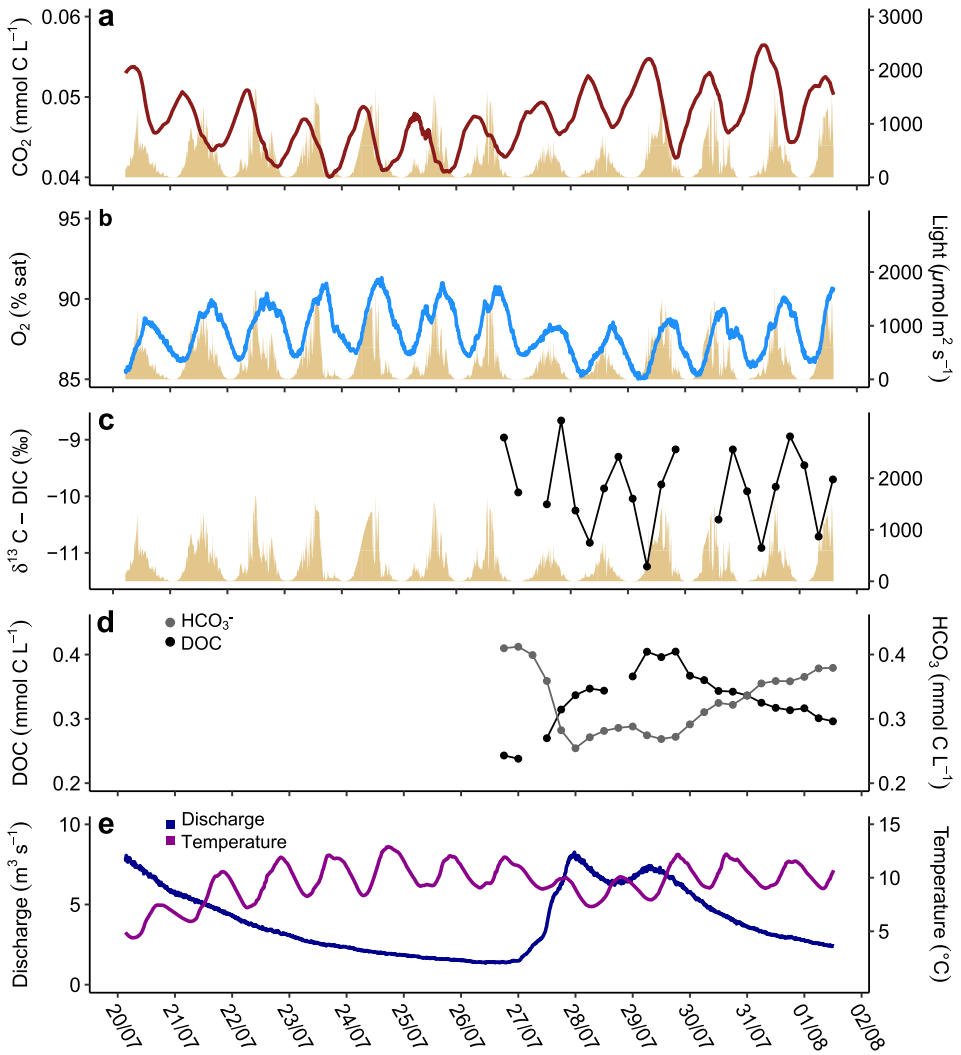

Fig. 2. Time series of stream solutes and physical properties in Kuparuk River. CO_2 (**a**), O_2 (**b**), discharge and temperature (**e**) were measured at 10-min intervals with sensors. δ^{13}CDIC (**c**), DOC and HCO_3 (**d**) were sampled every 6 h. In (**a**-**c**) light is shown as a secondary variable.

period. ER rates were higher than GPP, and therefore net ecosystem production (NEP; NEP = GPP − ER) was negative. NEP was -260 ± 52 mmol C m^{-2} d^{-1} in Kuparuk River compared to -61 ± 51 mmol C m^{-2} d^{-1} in Toolik River (Fig. 6). CO_2 evasion (E_{CO_2}) to the atmosphere was approximately twofold higher in the Kuparuk (323 ± 56 mmol C m^{-2} d^{-1}) compared to the Toolik River (186 ± 121 mmol C m^{-2} d^{-1}) and the mean contribution of stream NEP to CO_2 evasion (NEP/ $E_{CO_2} \times 100$) was 80% in Kuparuk River and 33% in Toolik River.

Discussion

The aim of this study was to assess the relative importance of biotic and abiotic processes in generating CO_2 emissions from tundra streams that drain continuous permafrost. We observed that CO_2 concentration decreased from night to day due to photosynthetic activity, which is inconsistent with the hypothesis that photo-oxidation is the primary mechanism generating CO_2 in these streams (Cory et al. 2014). Instead, the observed patterns suggest significant contributions of photosynthesis to stream diel CO_2 dynamics. This result concurs with observations from other Arctic streams (Rocher-Ros et al. 2020), as well as streams in other biomes (Peter et al. 2014; Crawford et al. 2016; Reiman and Jun Xu 2018). Furthermore, stream NEP was a major contributor to stream CO_2 evasion, with ER rates measured in situ that were 10 times greater than previously reported photo-oxidation rates from streams in the study region (Cory et al. 2014). Overall, in situ observations of dissolved C dynamics indicate that metabolic processes play a dominant role in CO_2 evasion from Arctic streams draining permafrost.

Light-dependent processes in Arctic streams

Our results showed a marked decrease of pCO_2 from night to day in Arctic streams (Figs. 2, 3) that can be explained by

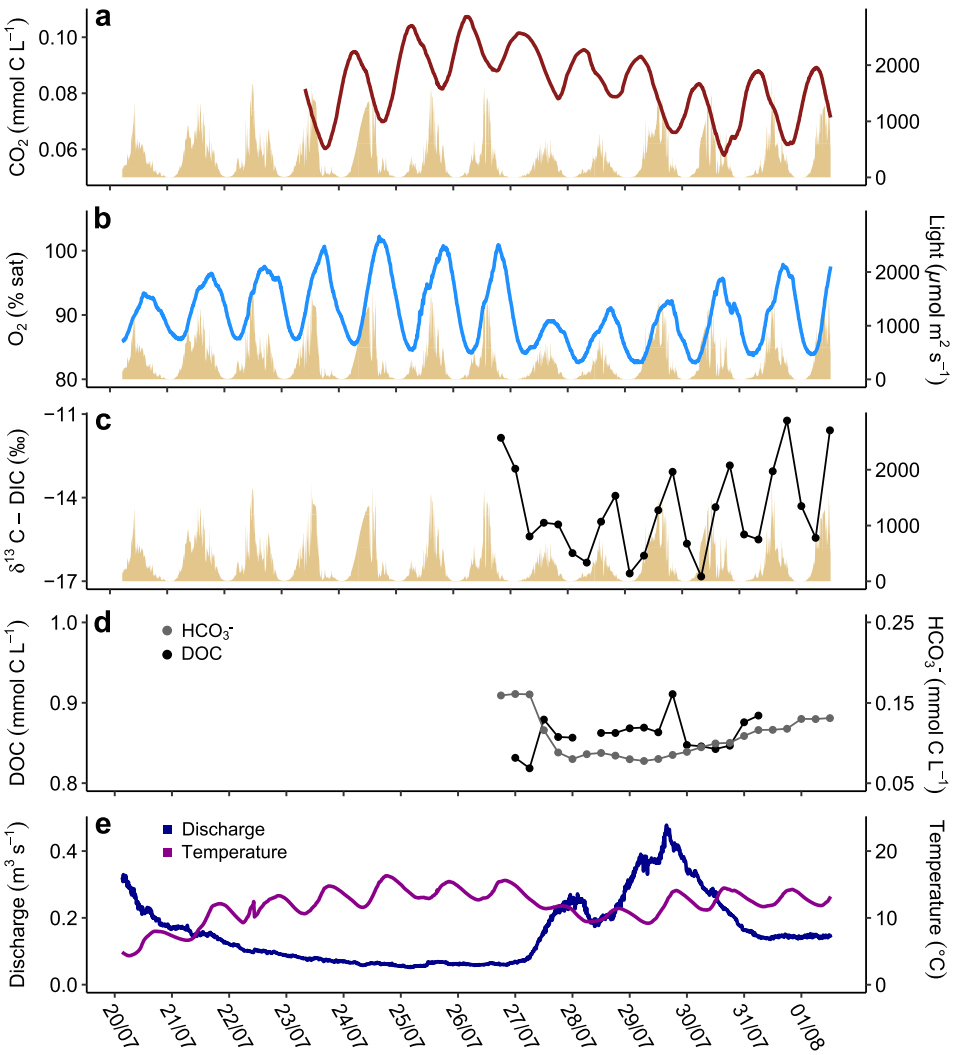

Fig. 3. Time series of stream solutes and physical properties in Toolik River. CO_2(**a**), O_2 (**b**), discharge and temperature (**e**) were measured at 10-min intervals with sensors. δ^{13}CDIC (**c**), DOC and HCO_3 (d) were sampled every 6 h. In (**a**-**c**) light is shown as a secondary variable.

stream photosynthetic activity (GPP) (Fig. 4a). In addition to a correlation between diurnal amplitude of dissolved CO_2 concentration and GPP, the role of photosynthesis is further supported by the strong positive relationship between the diel change in $\delta^{13}C_{DIC}$ and GPP (Fig. 4b). In both streams, average $\delta^{13}C_{DIC}$ values (−10‰ to −14.5‰) were more enriched than expected for DOC in these and other high-latitude streams, (~ −27‰; Peterson et al. 1993; Giesler et al. 2013). If photo-oxidation strongly influenced diel variation in $\delta^{13}C_{DIC}$, we would expect that the isotope values would be depleted and closer to $\delta^{13}C_{DOC}$ values during daytime (Fig. 1b, left panel). Instead, as CO_2 decreased during daytime, δ $^{13}C_{DIC}$ values increased, consistent with photosynthetic C-fixation as the primary driver of these dynamics (Fig. 1b, right panel). Thus, together, the metabolic rates derived from in situ O_2 mass-balance and changes in the isotopic composition of DIC strongly suggest that photosynthesis is an important light-dependent process in these streams that drives diel changes in CO_2 concentration and therefore evasion rates at sub-daily temporal scales.

Table 2. Physical and chemical properties of the streams. The mean value is shown with the interquartile range in parenthesis.

Site	Discharge (m^3 s^{-1})	Depth (m)	Temp. (°C)	Conductivity (μS cm^{-2})	pH	k_{600} (m d^{-1})
Kuparuk River	4.1 (2.3–6.2)	0.54 (0.49–0.63)	9.4 (8.4–10.9)	46.6 (42.6–51.3)	7.24 (6.99–7.42)	7.6 (7.1–8.4)
Toolik River	0.17 (0.07–0.23)	0.29 (0.18–0.39)	11.4 (9.6–13.5)	20.4 (16–26)	6.61 (6.50–6.71)	2.2 (1.1–2.7)

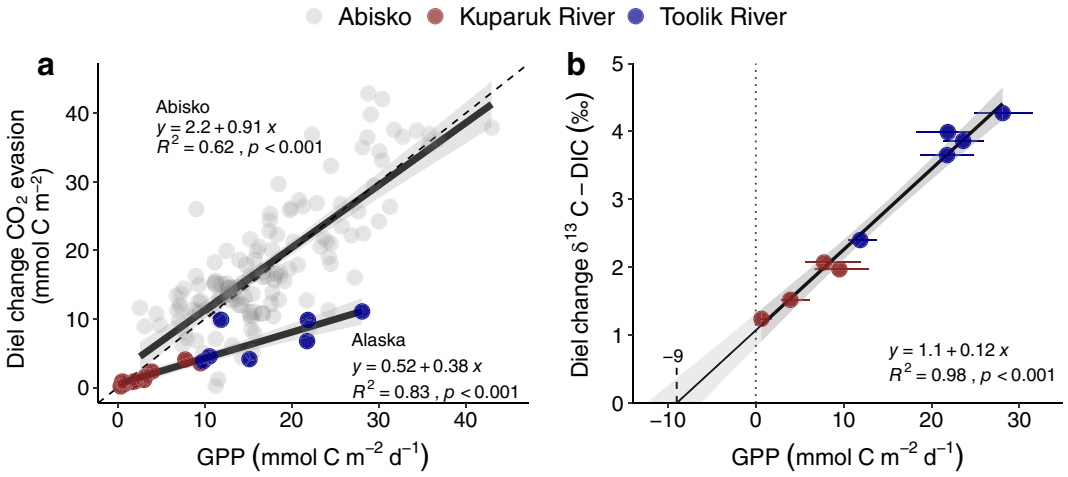

Fig. 4. Diel patterns of CO_2 evasion and $\delta^{13}C_{DIC}$ as a function of GPP. (**a**) Relationship between GPP and the absolute diel change in CO_2 evasion. The dashed line denotes the 1 : 1 line, and shown in gray is data from tundra streams in Abisko, Sweden, with similar K_{600} (Rocher-Ros et al. 2020). (**b**) Relationship between GPP and the day-night difference in $\delta^{13}C_{DIC}$. Note that the intercept with the y-axis is 1.1 and with the x-axis is −9 mmol C m^{-2} d^{-1} (95% confidence interval −12 to −6).

Relationships between GPP and diel patterns in CO_2 evasion and $\delta^{13}C_{DIC}$ values indicate a secondary role of photo-oxidation in generating CO_2 evasion from tundra streams. GPP does not solely explain the diel change in CO_2 evasion, which would require a 1 : 1 relationship between the two rates as observed in other Arctic streams (Rocher-Ros et al. 2020), but not in these Alaskan streams (Fig. 4a). Instead, the relationship deviated from 1 : 1, which could be caused by photo-oxidation of DOM. Photo-oxidation produces CO_2 during the day and therefore reduces the effect of the photosynthetic uptake of CO_2 (Fig. 1). Indeed, in both streams, we found a smaller diel amplitude in CO_2 evasion than expected from the effect of photosynthetic activity alone (Fig. 5). A significant diel change in $\delta^{13}C_{DIC}$ values occurred even when the modeled rate of GPP was zero (Fig. 4b), suggesting that photosynthesis may be occurring but not detectable based on diel changes in O_2. This may occur because photo-oxidation not only produces CO_2 but also consumes O_2 (Laane et al. 1985), and can therefore cause an underestimation of GPP derived from O_2 mass balance due to O_2 consumption by photo-oxidative reactions. The amount of C-fixation by photosynthesis but masked by photo-oxidation can be estimated from the x-intercept of the relationship between GPP and the diel change in $\delta^{13}C_{DIC}$ values, and thus represents an in situ estimate of photo-oxidation. This value was −9 mmol C m^{-2} d^{-1} (± 3), well within the range of laboratory-measured photo-oxidation rates for streams of the study region (Cory et al. 2014; Fig. 5), and similar to lakes elsewhere (Granéli et al. 1996; Koehler et al. 2014; Vachon et al. 2016). These findings suggest that combining whole-system estimates of metabolism with diel observations of CO_2 and $\delta^{13}C_{DIC}$ provides a promising approach for separating the relative role of light-dependent processes in streams.

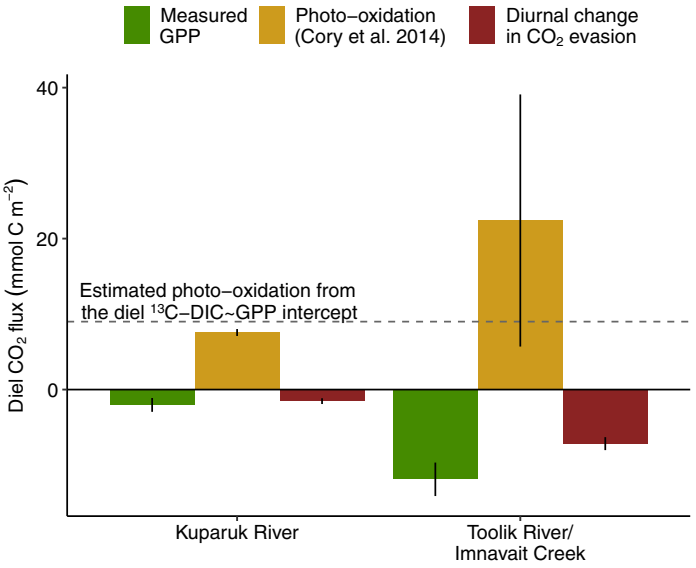

Fig. 5. CO_2 production and consumption by light-dependent processes in tundra streams. Green bars show GPP measured in this study in the Kuparuk and Toolik Rivers. Yellow bars represent the published photo-oxidation rates (Cory et al. 2014) in the Kuparuk River and in Imnavait Creek, an adjacent stream of similar size and DOC concentration to Toolik River. Red bars show the observed diel change in CO_2 evasion. Vertical black lines denote 1 standard error.

A more pronounced difference between GPP and the diel change in CO_2 evasion was observed in Toolik River than in the Kuparuk River (Figs. 4a, 5), which could also reflect the differences photo-oxidation. This pattern is consistent with laboratory results showing that photo-oxidation in the Kuparuk River was three times lower than in Imnavait Creek, an adjacent stream of similar size and DOC concentration as Toolik

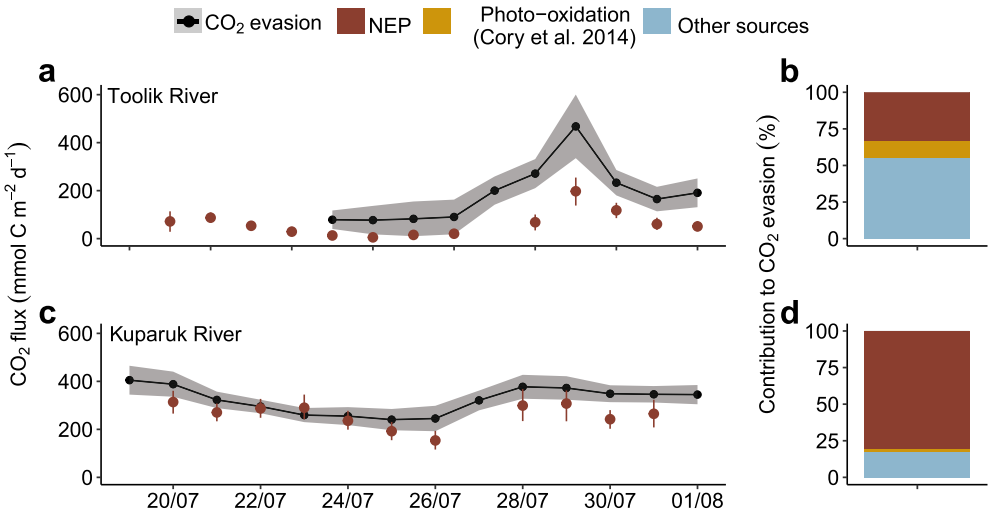

Fig. 6. Contribution of net ecosystem production (NEP) to CO_2 evasion. (**a**) and (**c**) show daily CO_2 evasion and NEP for Toolik River and Kuparuk River respectively. The shaded area for CO_2 evasion and the vertical lines for NEP represent 95% confidence intervals. (**b**) and (**d**) show mean contributions of NEP, photo-oxidation, and other sources to the measured CO_2 evasion for Toolik River and Kuparuk River, respectively, during the study period. Photo-oxidation rates are applied from the literature as described for Fig. 5.

River (Fig. 5; Cory et al. 2014; Fig. S1 for location). Such contrasts indicate that DOC concentration regulates the relative importance of photo-oxidation, as higher DOC can sustain higher photo-oxidation rates (Bertilsson and Tranvik 2000). This mechanism is further supported by contrasts between streams in Alaska and DOC-poor streams in Arctic Sweden. Across these sites, DOC is highest at Toolik River (10 mg C L^{-1}), lower in the Kuparuk River (4 mg C L^{-1}), and lowest in streams studied in arctic Sweden (below 2 mg C L^{-1}; Giesler et al. 2014). For the Swedish streams, photosynthesis clearly explains diel amplitude in CO_2 emissions with the data falling close to the 1 : 1 relationship, whereas the slope of this relationship is shallower for the streams in Alaska (Fig. 4a). We interpret these differences as an effect of photo-oxidation that produces CO_2 simultaneously with consumption by GPP (Fig. 1). Overall, these differences highlight the importance of DOC loading as a mediator of light-dependent processes in Arctic streams.

Sources of CO_2 evaded from Arctic streams

In situ estimates of CO_2 evasion and whole-stream metabolic rates suggested that photo-oxidation was not the major contributor to CO_2 evasion from the studied Arctic streams. Stream NEP was strongly negative (ER > GPP), comprising 80% of CO_2 evasion from the Kuparuk river and 33% from the Toolik River, whereas published rates of photo-oxidation cannot sustain CO_2 evasion observed from either river (Fig. 6b,d). This is in contrast to previous work that compared measured rates of photo-oxidation to modeled estimates of CO_2 evasion, concluding that 79–89% of CO_2 evasion from rivers and streams of the study region is generated by photo-oxidation (Cory et al. 2014). Estimates of metabolic rates made in the present study are consistent with previous estimates in Kuparuk River, with GPP rates ranging from 3 to 46 mmol C m^{-2} d^{-1} using benthic chambers (Peterson et al. 1986) and ER rates averaging 286 mmol C m^{-2} d^{-1} estimated using a two-station metabolism model (Bowden et al. 2014), and thus uncertainty in our estimates of NEP is unlikely to contribute to this discrepancy. Instead, the discrepancy between our study and Cory et al. (2014) likely occurred because the CO_2 evasion estimates from streams in this area in this study are an order of magnitude higher than rates assumed in the previous study. Evasion rates applied in the previous study (from Kling et al. 1991) were based on observed pCO_2 and an assumed gas transfer velocity that is consistent with lakes (0.5 m d^{-1}, Wanninkhof et al. 1985). Thus, although the dissolved pCO_2 in Kuparuk River was similar between our observations and those of Kling et al. (1991) (925 and 812 ppm, respectively) our estimates of CO_2 evasion for Kuparuk River are 27-fold greater because the rates of reaeration modeled from diurnal variation in dissolved O_2 were 14–17 times greater than those observed in lakes. Recent decades have seen important developments in research on gas transfer velocities in streams (Raymond et al. 2012; Ulseth et al. 2019; Hall and Ulseth 2020), which show the contribution of turbulent conditions to greater physical evasion rates from streams and rivers than lakes (Raymond et al. 2013).

NEP and photo-oxidation did not entirely account for CO_2 evasion from either river, although the unexplained flux was greater in Toolik River (55%) than in the Kuparuk River (17%). This unaccounted-for CO_2 suggests that additional processes are contributing to emissions (Fig. 6). Soil water inputs of CO_2 are a likely contributor, and are relatively greater in small, headwater streams than in larger rivers (Hotchkiss et al. 2015), consistent with the observed contrast in CO_2 emissions between the first- and fifth-order rivers. Additionally, we

observed more depleted $\delta^{13}C_{DIC}$ values during stormflows, consistent with a shift toward respiration of DOC produced in soils (Giesler et al. 2013; Figs. 3, 6). Thus, increased inputs of soil-derived CO_2 following storms could explain the observed temporal pattern, as shallow flowpaths are activated during storms (Rushlow and Godsey 2017) and contain elevated concentration of dissolved CO_2 (10,000–30,000 ppm in summer; (Pokrovsky et al. 2015; Harms et al. in review).

Responses of carbon processing to climate change in Arctic streams

Stream metabolism contributed significantly to CO_2 evasion in two Arctic streams draining continuous permafrost. CO_2 evasion to the atmosphere from fluvial ecosystems as a result of terrestrial inputs is a critical component of the C cycle (Raymond et al. 2013; Butman et al. 2015). In the Arctic, mobilization of previously stored organic C is ongoing due to climate change (Feng et al. 2013; Wauthy et al. 2018). Therefore, understanding and partitioning the relative importance of biotic and abiotic processes responsible for this large efflux are key to predicting how it might change under continued climate warming. Both photo-oxidation and photosynthesis are dependent on light, but biological processes are additionally sensitive to other factors, which could alter their overall balance. For instance, primary producers and therefore GPP in Arctic streams are sensitive to nutrients (Benstead et al. 2004; Slavik et al. 2004; Myrstener et al. 2018), temperature (Demars et al. 2016; Song et al. 2018), and disturbances (Parker & Huryn, 2013). Therefore, nutrient limitation (Slavik et al. 2004; Myrstener et al. 2018) or scouring floods (Roberts et al. 2007; Kendrick et al. 2019) likely constrain rates of GPP and may thereby sustain the relative importance of photo-oxidation as a driver of diel CO_2 patterns. In contrast, increased nutrient inputs from warming soils and thawing permafrost (Keuper et al. 2012; Kendrick et al. 2018; Harms et al. 2019) or declining summer flows (Brabets and Walvoord 2009; Bennett et al. 2015) might cause increased metabolic rates, whereas declining discharge-normalized DOC concentration (Kendrick et al. 2018) might reduce the relative contribution of photo-oxidation. We suggest that the future role of Arctic fluvial networks in the processing of C and CO_2 evasion will be largely dependent on how stream metabolic processes react to ongoing climate change.

References

Appling, A. P., R. O. Hall Jr., C. B. Yackulic, and M. Arroita. 2018. Overcoming equifinality: Leveraging long time series for stream metabolism estimation. J. Geophys. Res. Biogeo. **123**: 624–645. doi:10.1002/2017JG004140

Battin, T. J., L. a. Kaplan, S. Findlay, C. S. Hopkinson, E. Marti, A. I. Packman, J. D. Newbold, and F. Sabater. 2008. Biophysical controls on organic carbon fluxes in fluvial networks. Nat. Geosci. **1**: 95–100. doi:10.1038/ngeo101

Bennett, K. E., A. J. Cannon, and L. Hinzman. 2015. Historical trends and extremes in boreal Alaska river basins. J. Hydrol. **527**: 590–607. doi:10.1016/j.jhydrol.2015.04.065

Benstead, J. P., and others. 2004. Responses of a beaded Arctic stream to short-term N and P fertilisation. Freshw. Biol. **50**: 277–290. doi:10.1111/j.1365-2427.2004.01319.x

Berggren, M., J. F. Lapierre, and P. A. Del Giorgio. 2012. Magnitude and regulation of bacterioplankton respiratory quotient across freshwater environmental gradients. ISME J. **6**: 984–993. doi:10.1038/ismej.2011.157

Bertilsson, S., and L. J. Tranvik. 2000. Photochemical transformation of dissolved organic matter in lakes. Limnol. Oceanogr. **45**: 753–762. doi:10.4319/lo.2000.45.4.0753

Bowden, W. B., and others. 2014. Ecology of streams of the Toolik region, p. 173–237. *In* Alaska's changing arctic. Oxford Univ. Press.

Brabets, T. P., and M. A. Walvoord. 2009. Trends in streamflow in the Yukon River Basin from 1944 to 2005 and the influence of the Pacific Decadal Oscillation. J. Hydrol. **371**: 108–119. doi:10.1016/j.jhydrol.2009.03.018

Butman, D., S. Stackpoole, E. Stets, C. P. Mcdonald, D. W. Clow, and R. G. Striegl. 2015. Aquatic carbon cycling in the conterminous United States and implications for terrestrial carbon accounting. Proc. Natl. Acad. Sci. **1–6**: 58–63. doi:10.1073/pnas.1512651112

Campeau, A., M. B. Wallin, R. Giesler, S. Löfgren, C. M. Mörth, S. Schiff, J. J. Venkiteswaran, and K. Bishop. 2017. Multiple sources and sinks of dissolved inorganic carbon across Swedish streams, refocusing the lens of stable C isotopes. Sci. Rep. **7**: 1–14. doi:10.1038/s41598-017-09049-9

Cherry, J. E., S. J. Déry, Y. Cheng, M. Stieglitz, A. S. Jacobs, and F. Pan. 2014. Climate and hydrometeorology of the Toolik Lake region and the Kuparuk River basin, p. 21–60. *In* Alaska's changing arctic. Oxford Univ. Press.

Cole, J. J., and N. F. Caraco. 2001. Carbon in catchments: Connection terrestrial losses to aquatic metabolism. Mar. Freshw. Res. **52**: 101–110. doi:10.1071/MF00084

Cory, R. M., C. P. Ward, B. C. Crump, and G. W. Kling. 2014. Sunlight controls water column processing of carbon in arctic fresh waters. Science **345**: 925–928. doi:10.1126/science.1253119

Crawford, J. T., E. H. Stanley, M. M. Dornblaser, and R. G. Striegl. 2016. CO_2 time series patterns in contrasting headwater streams of North America. Aquat. Sci. **79**: 473–486. doi:10.1007/s00027-016-0511-2

Demars, B. O. L., G. M. Gíslason, J. S. Ólafsson, J. R. Manson, N. Friberg, J. M. Hood, J. J. D. Thompson, and T. E. Freitag. 2016. Impact of warming on CO_2 emissions from streams countered by aquatic photosynthesis. Nat. Geosci. **9**: 758–761. doi:10.1038/NGEO2807

Feng, X., and others. 2013. Differential mobilization of terrestrial carbon pools in Eurasian Arctic river basins. Proc. Natl. Acad. Sci. USA **110**: 14168–14173. doi:10.1073/pnas.1307031110

Giesler, R., S. W. Lyon, C.-M. C.-M. Mörth, J. Karlsson, E. M. Karlsson, E. J. Jantze, G. Destouni, and C. Humborg. 2014. Catchment-scale dissolved carbon concentrations and export estimates across six subarctic streams in northern Sweden. Biogeosciences **11**: 1–15. doi:10.5194/bg-11-1-2014

Giesler, R., C. Mörth, J. Karlsson, E. J. Lundin, S. W. Lyon, and C. Humborg. 2013. Spatiotemporal variations of pCO_2 and δ13C-DIC in subarctic streams in northern Sweden. Global Biogeochem. Cycles **27**: 176–186. doi:10.1002/gbc.20024

Grace, M. R., D. P. Giling, S. Hladyz, V. Caron, R. M. Thompson, and R. Mac Nally. 2015. Fast processing of diel oxygen curves: Estimating stream metabolism with base (Bayesian single-station estimation). Limnol. Oceanogr.: Methods **13**: 103–114. doi:10.1002/lom.10011

Granéli, W., M. Lindell, and L. Tranvik. 1996. Photo-oxidative production of dissolved inorganic carbon in lakes of different humic content. Limnol. Oceanogr. **41**: 698–706. doi:10.4319/lo.1996.41.4.0698

Guy, R. D., M. L. Fogel, and J. A. Berry. 1993. Photosynthetic fractionation of the stable isotopes of oxygen and carbon. Plant Physiol. **101**: 37–47. doi:10.1104/pp.101.1.37

Hall, R. O., and E. R. Hotchkiss. 2017. Stream metabolism. Elsevier Inc.

Hall, R. O., J. L. Tank, M. A. Baker, E. J. Rosi-Marshall, and E. R. Hotchkiss. 2015. Metabolism, gas exchange, and carbon spiraling in rivers. Ecosystems **19**: 73–86. doi:10.1007/s10021-015-9918-1

Hall, R. O., and A. J. Ulseth. 2020. Gas exchange in streams and rivers. WIREs Water **7**: 1–18. doi:10.1002/wat2.1391

Hanson, P. C., S. R. Carpenter, N. Kimura, C. Wu, S. P. Cornelius, and T. K. Kratz. 2008. Evaluation of metabolism models for free-water dissolved oxygen methods in lakes. Limnol. Oceanogr.: Methods **6**: 454–465. doi:10.4319/lom.2008.6.454

Harms, T. K., C. L. Cook, A. N. Wlostowski, M. N. Gooseff, and S. E. Godsey. 2019. Spiraling down hillslopes: Nutrient uptake from water tracks in a warming Arctic. Ecosystems **22**: 1546–1560. doi:10.1007/s10021-019-00355-z

Hornberger, G. M., and M. G. Kelly. 1975. Atmospheric reaeration in a river using productivity analysis. J. Environ. Eng. Div. **101**: 729–739.

Hotchkiss, E. R., and R. O. J. Hall. 2014. High rates of daytime respiration in three streams: Use of $\delta^{18}O_{O2}$ and O_2 to model diel ecosystem metabolism. Limnol. Oceanogr. **59**: 798–810. doi:10.4319/lo.2014.59.3.0798

Hotchkiss, E. R., R. O. Hall, R. Sponseller, D. Butman, J. Klaminder, H. Laudon, M. Rosvall, and J. Karlsson. 2015. Sources and control of CO_2 emissions change with the size of sreams and rivers. Nat. Geosci. **8**: 696–699.

Huryn, A. A. D., J. P. J. Benstead, and S. S. M. Parker. 2014. Seasonal changes in light availability modify the temperature dependence of ecosystem metabolism in an arctic stream. Ecology **95**: 2826–2839. doi:10.1890/13-1963.1

Kendrick, M. R., A. E. Hershey, and A. D. Huryn. 2019. Disturbance, nutrients, and antecedent flow conditions affect macroinvertebrate community structure and productivity in an Arctic river. Limnol. Oceanogr. **64**: S93–S104. doi:10.1002/lno.10942, S1

Kendrick, M. R., and others. 2018. Linking permafrost thaw to shifting biogeochemistry and food web resources in an arctic river. Glob. Chang. Biol. **24**: 5738–5750. doi:10.1111/gcb.14448

Keuper, F., P. M. van Bodegom, E. Dorrepaal, J. T. Weedon, J. van Hal, R. S. P. van Logtestijn, and R. Aerts. 2012. A frozen feast: Thawing permafrost increases plant-available nitrogen in subarctic peatlands. Glob. Chang. Biol. **18**: 1998–2007. doi:10.1111/j.1365-2486.2012.02663.x

Kling, G. W., G. W. Kipphut, and M. C. Miller. 1991. Arctic lakes and streams as gas conduits to the atmosphere: Implications for tundra carbon budgets. Science **251**: 298–301. doi:10.1126/science.251.4991.298

Koehler, B., T. Landelius, G. A. Weyhenmeyer, N. Machida, and L. J. Tranvik. 2014. Sunlight-induced carbon dioxide emissions from inland waters. Global Biogeochem. Cycles **28**: 696–711. doi:10.1002/2014GB004850

Laane, R. W. P. M., W. W. C. Gieskes, G. W. Kraay, and A. Eversdijk. 1985. Oxygen consumption from natural waters by photo-ixidizing processes. Neth. J. Sea Res. **19**: 125–128.

Miles, C. J., and P. L. Brezonik. 1981. Oxygen consumption in humic-colored waters by a photochemical ferrous-ferric catalytic cycle. Environ. Sci. Technol. **15**: 1089–1095. doi:10.1021/es00091a010

Miller, W. L., and R. G. Zepp. 1995. Photochemical production of dissolved inorganic carbon from terrestrial organic matter: Significance to the oceanic organic carbon cycle. Geophys. Res. Lett. **22**: 417–420. doi:10.1029/94GL03344

Moore, R. D. D. 2005. Slug injection using salt in solution. Streamline Watershed Manag. Bull **8**: 1–6.

Myrstener, M., G. Rocher-Ros, R. M. Burrows, A.-K. Bergström, R. Giesler, and R. A. Sponseller. 2018. Persistent nitrogen limitation of stream biofilm communities along climate gradients in the Arctic. Glob. Chang. Biol. **24**: 3680–3691. doi:10.1111/gcb.14117

Odum, H. T. 1956. Primary production in flowing waters. Limnol. Oceanogr. **1**: 102–117. doi:10.4319/lo.1956.1.2.0102

Opsahl, S. P., and R. G. Zepp. 2001. Photochemically-induced alteration of stable carbon isotope ratios ($\delta^{13}C$) in terrigeneous dissolved organic carbon. Geophys. Res. Lett. **28**: 2417–2420. doi:10.1029/2000GL012686

Osburn, C. L., D. P. Morris, K. A. Thorn, and R. E. Moeller. 2001. Chemical and optical changes in freshwater dissolved organic matter exposed to solar radiation. Biogeochemistry **54**: 251–278. doi:10.1023/A:1010657428418

Parker, S. M., and A. D. Huryn. 2013. Disturbance and productivity as codeterminants of stream food web complexity in the Arctic. Limnol. Oceanogr. **58**: 2158–2170. doi:10.4319/lo.2013.58.6.2158

Parker, S. R., S. R. Poulson, C. H. Gammons, and M. D. Degrandpre. 2005. Biogeochemical controls on diel cycling of stable isotopes of dissolved O_2 and dissolved inorganic carbon in the Big Hole River, Montana. Environ. Sci. Technol. **39**: 7134–7140. doi:10.1021/es0505595

Parkhurst, D. L., and C. A. J. Appelo. 2013. PHREEQC (version 3)—a computer program for speciation, batch-reaction, one-dimensional transport, and inverse geochemical calculations. Model. Tech. B **6**: 99-4259.

Peter, H., G. A. Singer, C. Preiler, P. Chifflard, G. Steniczka, and T. J. Battin. 2014. Scales and drivers of temporal pCO_2 dynamics in an Alpine stream. J. Geophys. Res. Biogeo. **119**: 1078–1091. doi:10.1002/2013JG002552

Peterson, B., B. Fry, L. Deegan, and A. Hershey. 1993. The trophic significance of epilithic algal production in a fertilized tundra river ecosystem. Limnol. Oceanogr. **38**: 872–878. doi:10.4319/lo.1993.38.4.0872

Peterson, B. J., J. E. Hobbie, and T. L. Corliss. 1986. Carbon flow in a tundra stream ecosystem. Can. J. Fish. Aquat. Sci. **43**: 1259–1270. doi:10.1139/f86-156

Pokrovsky, O. S., and others. 2015. Permafrost coverage, watershed area and season control of dissolved carbon and major elements in western Siberian rivers. Biogeosciences **12**: 6301–6320. doi:10.5194/bg-12-6301-2015

R Core Team. 2017. R: A language and environment for statistical computing.

Raymond, P. A., and others. 2013. Global carbon dioxide emissions from inland waters. Nature **503**: 355–359. doi:10.1038/nature12760

Raymond, P. A., and others. 2012. Scaling the gas transfer velocity and hydraulic geometry in streams and small rivers. Limnol. Oceanogr.: Fluids and Environments **2**: 41–53. doi:10.1215/21573689-1597669

Reiman, J. H., and Y. Jun Xu. 2018. Diel variability of pCO_2 and CO_2 outgassing from the lower Mississippi River: Implications for riverine CO_2 outgassing estimation. Water **11**: 1–15. doi:10.3390/w11010043

Roberts, B. J., P. J. Mulholland, and W. R. Hill. 2007. Multiple scales of temporal variability in ecosystem metabolism rates: Results from 2 years of continuous monitoring in a forested headwater stream. Ecosystems **10**: 588–606. doi:10.1007/s10021-007-9059-2

Rocher-Ros, G., R. A. Sponseller, A. Bergström, M. Myrstener, and R. Giesler. 2020. Stream metabolism controls diel patterns and evasion of CO_2 in Arctic streams. Glob. Chang. Biol. **26**: 1400–1413. doi:10.1111/gcb.14895

Rushlow, C. R., and S. E. Godsey. 2017. Rainfall—runoff responses on Arctic hillslopes underlain by continuous permafrost, North Slope, Alaska, USA. Hydrol. Process. **31**: 4092–4106. doi:10.1002/hyp.11294

Schindler, D. E., K. Jankowski, Z. T. A'mar, and G. W. Holtgrieve. 2017. Two-stage metabolism inferred from diel oxygen dynamics in aquatic ecosystems. Ecosphere **8**: e01867. doi:10.1002/ecs2.1867

Shaver, G. R., and others. 2014. Terrestrial ecosystems at Toolik Lake, Alaska, p. 90–142. *In* Alaska's changing Arctic. Oxford Univ. Press.

Slavik, K., B. J. Peterson, L. A. Deegan, W. B. Bowden, A. E. Hershey, and J. E. Hobbie. 2004. Long-term response of the Kuparuk River ecosystem to phosphorus fertilization. Ecology **85**: 939–954. doi:10.1890/02-4039

Song, C., and others. 2018. Continental-scale decrease in net primary productivity in streams due to climate warming. Nat. Geosci. **11**: 415–420. doi:10.1038/s41561-018-0125-5

Spencer, R. G. M., P. J. Mann, T. Dittmar, T. I. Eglinton, C. McIntyre, R. M. Holmes, N. Zimov, and A. Stubbins. 2015. Detecting the signature of permafrost thaw in Arctic rivers. Geophys. Res. Lett. **42**: 2830–2835. doi:10.1002/2015GL063498

Stackpoole, S. M., D. E. Butman, D. W. Clow, K. L. Verdin, B. V. Gaglioti, H. Genet, and R. G. Striegl. 2017. Inland waters and their role in the carbon cycle of Alaska. Ecol. Appl. **27**: 1403–1420. doi:10.1002/eap.1552

Taipale, S. J., and E. Sonninen. 2009. The influence of preservation method and time on the $\delta^{13}C$ value of dissolved inorganic carbon in water samples. Rapid Commun. Mass Spectrom. **23**: 2507–2510.

Thimijan, R., and R. Heins. 1983. Photometric, radiometric, and quantum light units of measure: A review of procedures for interconversion. HortScience **18**: 818–822.

Toolik Field Station, Institute of Arctic Biology. 2019. Environmental Data Center Team. Meteorological monitoring program at Toolik, Alaska.

Tranvik, L. 1988. Availability of dissolved organic carbon for planktonic bacteria in oligotrophic lakes of differing humic content. Microb. Ecol. **16**: 311–322.

Ulseth, A. J., R. O. Hall Jr., M. B. Canadell, H. L. Madinger, A. Niayifar, and T. J. Battin. 2019. Distinct air–water gas exchange regimes in low- and high-energy streams. Nat. Geosci. **1**: 259–263. doi:10.1038/s41561-019-0324-8

Vachon, D., J. Lapierre, and P. A. Giorgio. 2016. Seasonality of photochemical dissolved organic carbon mineralization and its relative contribution to pelagic CO_2 production in northern lakes. Biogeosciences **121**: 864–878. doi:10.1002/2015JG003244

Waldron, S., E. M. Scott, and C. Soulsby. 2007. Stable isotope analysis reveals lower-order river dissolved inorganic carbon pools are highly dynamic. Environ. Sci. Technol. **41**: 6156–6162. doi:10.1021/es0706089

Wanninkhof, R., J. R. Ledwell, and W. S. Broecker. 1985. Gas exchange-wind speed relation measured with sulfur hexafluoride on a lake. Science (80) **227**: 1224–1226. doi:10.1126/science.227.4691.1224

Wauthy, M., M. Rautio, K. S. Christoffersen, L. Forsström, I. Laurion, H. L. Mariash, S. Peura, and W. F. Vincent. 2018. Increasing dominance of terrigenous organic matter in circumpolar freshwaters due to permafrost thaw. Limnol. Oceanogr.: Lett. **3**: 186–198. doi:10.1002/lol2.10063

Wild, B., and others. 2019. Rivers across the Siberian Arctic unearth the patterns of carbon release from thawing permafrost. Proc. Natl. Acad. Sci. USA **116**: 10280–10285. doi: 10.1073/pnas.1811797116

Zolkos, S., S. E. Tank, R. G. Striegl, and S. V. Kokelj. 2019. Thermokarst effects on carbon dioxide and methane fluxes in streams on the Peel Plateau (NWT, Canada). J. Geophys. Res. Biogeo. **124**: 1781–1798. doi:10.1029/2019JG005038

Acknowledgments

The authors thank Albin Bjärhall for the help in the field and the lab. The authors are grateful to the Toolik Field Station for support and the Arctic Long-Term Ecological Research Program for meteorological data. This study was supported by the Swedish Research Council (VR; 2013-5001), the Swedish Research Council for Environment, Agricultural Sciences, and Spatial Planning (FORMAS; 2014-00970) and INTERACT (Grant Agreement No. 730938) and INTERACT Transnational Access to R.G. The authors thank two anonymous reviewers that provided insightful comments to a previous version of this manuscript.

Conflict of Interest

None declared.

Submitted 23 January 2020
Revised 09 June 2020
Accepted 30 June 2020